HYPERSONIC ENGINE AIRPLANE INTEGRATION

(NASA-CR-143376) HYPERSONIC ENGINE AIRPLANE INTEGRATION Progress Report, 1 Feb. - 1 Sep. 1975 (New York Univ.) 20 p HC $3.25 CSCL 20E

N75-30174

Unclas
G3/07 34265

NEW YORK UNIVERSITY
DIVISION OF APPLIED SCIENCE
AEROSPACE AND ENERGETICS LABORATORY
MERRICK AND STEWART AVENUES
WESTBURY, L.I.N.Y. 11590 NEW YORK

PROGRESS REPORT

February 1, 1975 through September 1, 1975

NASA GRANT NGR-33-016-131

SEPTEMBER, 1975

A summary of the research activities conducted during the above period at the New York University Aerospace and Energetics Laboratory under the referenced Grant is presented here.

Research on this Grant is concerned with the design and analysis of an integrated scramjet engine that utilizes heat conduction flames. The scramjet engine model described in the last progress report (August 1, 1975 through February 1, 1975) was tested at a freestream Mach number of 4.0 by personnel at the General Applied Science Laboratory. The research effort during the above period was primarily concerned with the interpretation and analysis of the experimental data. The mixing tests were conducted with cold ambient air (T_o = 530°R and p_o = 60 psia). While the conbustion tests were conducted with hot vitiated air ($T_o \sim 1800$°R and $p_o \sim 120$ psia).

The purpose of the cold mixing tests was to determine the degree of mixedness of the fuel at the ignitor station so as to certify if the fuel injection conditions (M_j) and fuel injectors locations were properly selected to give a uniform fuel concentration profile at the ignitor station. A second objective of these these was to assess the influence of the fuel injection on the inlet flow. Several fuel injection configurations were tested. An analysis of some of these tests has been documented in an internal memorandum which is due to be incorporated in the final report. A summary of some results is given here.

Inlet Tests

Figure 1 gives the measured static pressure along the upper surface, the lower (cowl) surface, and at various stations on the inlet sidewalls with and without fuel injection. The measured

hydrogen concentration, pitot pressure and static pressure profiles at the ignitor station are shown in Fig. 2 along with the deduced Mach number, local recovery and streamtube contraction profiles.

The measurements without fuel injection indicate that the inlet flow field is significantly influenced by the presence of the fuel injectors. The nominal expected 65% inviscid inlet recovery is measured to be about 35% (Fig. 2). Correspondingly the maximum static pressure rise is also reduced significantly (Fig. 1) $\left[\frac{p}{p_\infty} = \left(\frac{p}{p_o}\right)\left(\frac{p_o}{p_{o\infty}}\right)\frac{p_{o\infty}}{p_\infty}\right]$. The capture area is determined from the local streamtube contract to be approximately 62% as opposed to the expected 78.5%. These differences are mostly due to the fact that the freestream fuel injectors had to be constructed sturdier than envisioned in the design phase to insure their structural integrity. The freestream injectors are each 0.60" thick as compared to the 6.0" cowl height or worse with the 4.7" captured streamtube height. The bow shock alone produced by these injectors cause a 20% loss in both recovery and capture area. The wake from these injectors produces additional losses. Also wave diagrams using the actual configuration tested indicate that the shock waves produced by the fuel injection system coalesce and strengthen other shock waves in the flow field. While the expansion waves produce increased in the local Mach number upstream of the shock waves thereby causing large stagnation pressure losses. Furthermore with certain injection conditions, reversed flow field and separation bubbles can be formed when mixing occurs in strong adverse pressure gradient regions.

To avoid these undesirable events, the following injection criteria were deduced: First the stagnation pressure of the injected fuel should

be greater than that of the maximum static pressure rise encountered divided by the inlet recovery. Second to avoid reverse flow in the mixing layers, the injection Mach number should be such that the momentum of the injected fuel is greater than the inlet drag since this is the same force that is applied to decelerate the captured fluid. By application of the momentum conservation, this criterior leads to

$$M_j^2 \geq \frac{1}{2\gamma}\left[\left(\frac{p_{max}}{p_\infty} - 1\right)\left(\frac{A_{min}}{A_\infty} + 1\right)\right]$$

Where A_{min}/A_∞ is the inlet aerodynamic contraction ratio. To avoid subsonic flow regions in the mixing layer

$$M_j^2 \geq \frac{1}{2\gamma}\left[\left(\frac{p_{max}}{p_\infty} - 1\right)\left(\frac{A_{min}}{A_\infty}\right) + \gamma\left(\frac{p_{max}}{p_\infty}\right)\left(\frac{A_{min}}{A_\infty}\right)\right]$$

For the present test conditions this means injection Mach numbers greater than 3. The use of weak oblique shocks in the inlet and nearly matched injection pressure are helpful in avoiding these effects.

The above results indicate the need for more efficient inlet and fuel injector system. A greater diffusion level and higher static pressure may be had by increasing the inlet contraction; however, at the rise of not being able to start the inlet since it is two-dimensional. An additional draw-back of the present inlet is the rapid pressure drop experienced downstream of the throat. This is produced by the 12^o expansion corner on the upper surface. It causes the static pressure at the ignitor station to drop to about 6 times the freestream level and the local Mach number there to increase to 2.1. This expansion is much too rapid for the combustion; therefore shoud be reduced. Also

the ignition should be moved slightly upstream.

Mixing Tests

When fuel is injected as in test 44C (Fuel injection through the cowl injector #1, the midstream injector #2, and the lower freestream injector so that the global equivalence ratio is approximately 0.9), the mean recovery is reduced to approximately 25%. There is a slight increase in the static pressure and the Mach number at the ignitor station is reduced to approximately 1.8. The capture area is also reduced slightly to 58% due to the streamline displacement effects of the freestream injectors.

The measured hydrogen concentration profiles for this test is shown in Fig. 2 also. This shows that the fuel concentration profile peaks close to the cowl (lower) surface since no fuel was injected from either the upper freestream injector or the surface injector. Fuel injection through these was found to aggravate a small separation pocket near the inlet of the boundary layer scoop. Nonetheless the profile shows a fairly well mixed fuel air profile.

An analysis of the mixing at the actual test conditions, when fuel is injected through the midstream injector only is shown in Fig. 3 for different eddy viscosity levels. The measured values are also shown. These indicate an eddy viscosity level of about 1×10^{-4} to 1×10^{-3} is correct for the present conditions.

The good agreement observed for this case is encouraging in view of the complex flowfield considered. Analysis for each injector separately were conducted for the actual test conditions used. The results are reported in the internal memorandum. The effects of adjacent injectors and of the boundary layer on the inlet and cowl surfaces was not

considered. The analysis of the complete configuration, i.e., injection through several injectors is more complex. However a study of the measured concentration profiles with different fuel injection configurations, reveals that to a certain extent the individual contributions of the separate injectors concentration profile can be superimposed to produce the total profile. More detailed experimental data and a comprehensive theoretical analysis of this flowfield is needed to delineate the limits of superposition and to determine the interaction effects of adjacent injectors. The effects of the boundary layer on the mixing is presently being investigated for the cowl injector.

Combustion Tests: The combustion tests were conducted with nominal fuel injection similar to those described above so that the hydrogen concentration profile at the ignitor station is similar to the one presented above. The combustor wall, however, was modified in order to increase the static pressure level in the combustor. The modification was made by inserting an 8^{o} wedge on the lower surface (Fig. 6). Several tests with different freestream stagnation temperatures and fuel distribution were made. With the above conditions (i.e. local flow velocity of nominally 3100 ft/sec, $T_{o\infty} \approx 1700^{o}R$, $p_{local} = 6$ psia). The local combustion produced by the ignitor did not sustain itself. An analysis of test #80 which is typical of these conditions showed that the induction and reaction times are large at these conditions so that the diffusion effects quench the flame. This is evident from a study of Fig. 4a where the measured stagnation temperature profile at the combustor exit is compared to the theoretically calculated ones assuming two different levels of viscosity. The stagnation temperature variation along the lower wall calculated

assuming no heat transfer there is presented in Fig. 4b for the two cases. The measured experimental values are also indicated. This shows that with the low viscosity level there is an ignition delay of .05 milliseconds after which the temperature increases. While the higher viscosity the temperature decreases continuously.

In test #82, the local flow velocity was reduced to 2500 ft/sec corresponding to a local Mach number close to 1.2, and the freestream stagnation temperature was increased to approximately 2000°R. At these conditions the pilot flame sustained itself as evident from Fig. 5 where the measured stagnation temperature profiles at the combustor exit ($x \approx .9$ ft) before and after ignition are shown. A radiation loss correction was applied to this data since the thermocouples were unshielded. A theoretical analysis of the combustion at these conditions was undertaken to determine the flowfield characteristics. The initial conditions (Mach number, temperature and concentration) were reconstructed from a test with similar inlet flow and from the measured injected hydrogen mass flow rate.

The calculated stagnation temperature profile usinga high level of viscosity is shown in Fig. 5. The flow conditions used are indicated in the figure. The corresponding isotherms, edge of mixing and combustion and a typical streamline passing through the flame at the combustor exit are shown in Fig. 6. The measured static pressure variation along the upper and lower surfaces of the combustor walls are shown at the botton of Fig. 6. The mean curve fit shown in the figure was used in the analysis. The fact that the pressure on both surfaces are nearly the same is consistent with the low supersonic speed and the rather thick

flame (large reaction time) prevailent at these conditions. The flame thickness increases downstream of the ignitor due to the favorable pressure gradient. The measured variation of temperature along the lower surface is shown in Fig. 7. The ignition delay is evident in this figure by the initial decrease in temperature along with the theoretical curve assuming no heat transfer at the wall.

The mean flame angle defined here as

$$\text{Tan } \theta_f = \frac{y_i - y_o}{x_i - x_o}$$

where y is the height from the surface of the inflection point in the temperature porfile at a station x_i and y_o is that corresponding one at a station x_o. For these conditions a mean flame angle of approximately 9^o is evident. This compares rather favorably with the experimental and theoretical correlations of premixed turbulent flame angles shown in Fig. 8.

The streamline shown in Fig. 6 indicates that approximately one third of the captured flow has passed through the flame. A stagnation pressure ratio across this combustion of 0.5 is indicated by the analysis. The effects of the boundary layer on this combustion are being estimated.

In conclusion, it has been demonstrated that a stable and fairly rapid premixed heat conduction type flame can be sustained at a freestream Mach number of 4.0 when the diffusion Mach number is on the order of 1.2. With the present conditions, the reaction times and diffusion times are comparable so that a thick flame is produced with negligible lateral pressure gradients. An increase in the local flow speed and associated

reduction in static pressure and temperature produce reaction times greater that are greater than the diffusion time so that the flame cannot sustain itseif. In either case, the theoretical analysis describes the flowfield fairly accurately when the correct level of viscosity is employed.

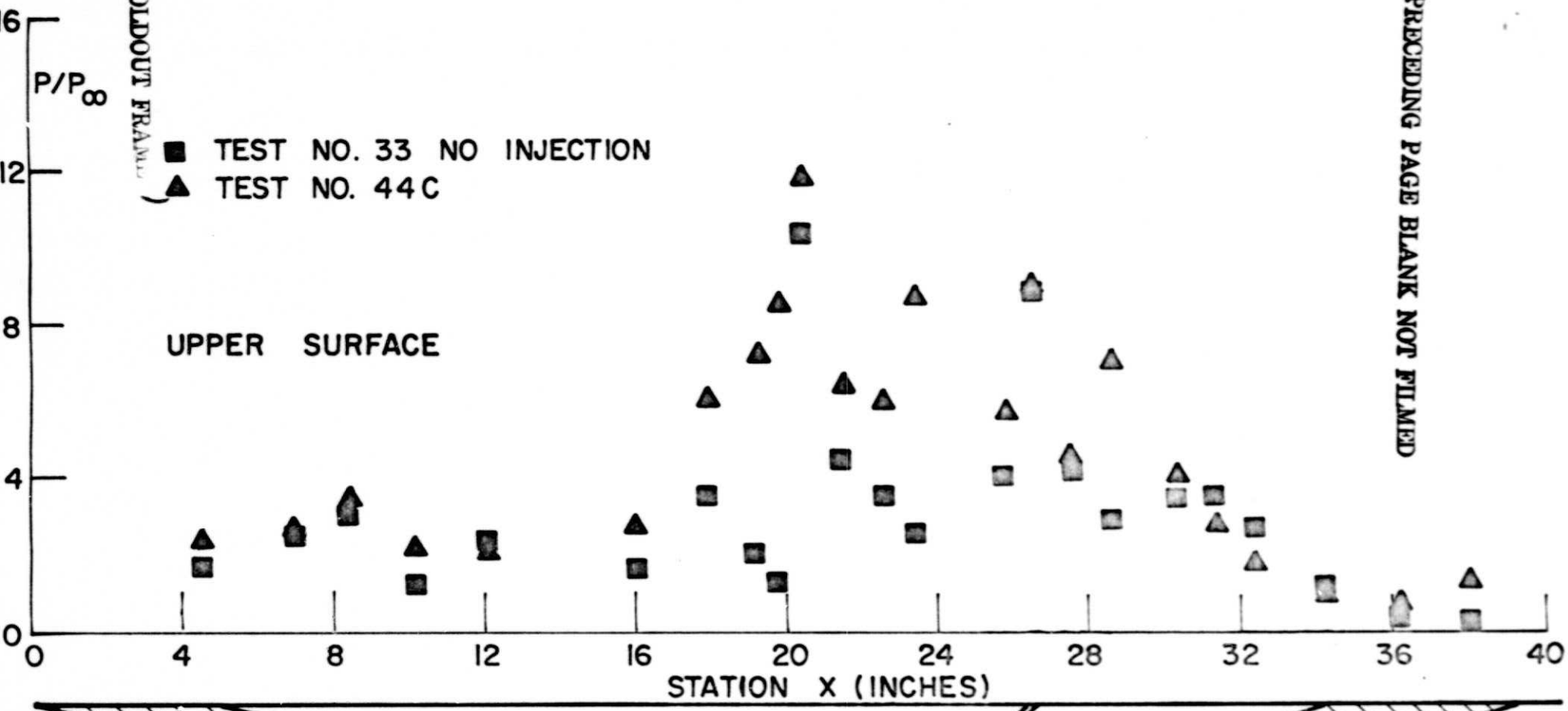

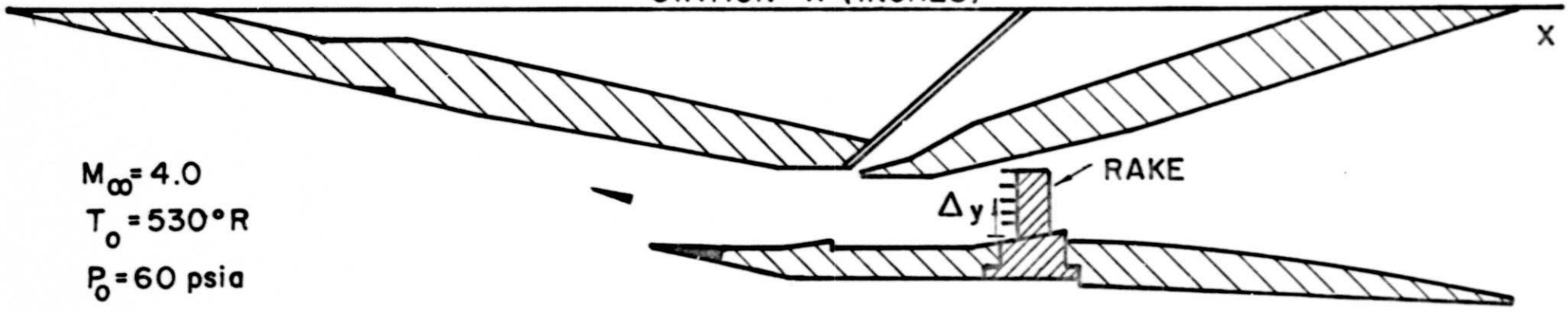

$M_\infty = 4.0$

$T_0 = 530°R$

$P_0 = 60$ psia

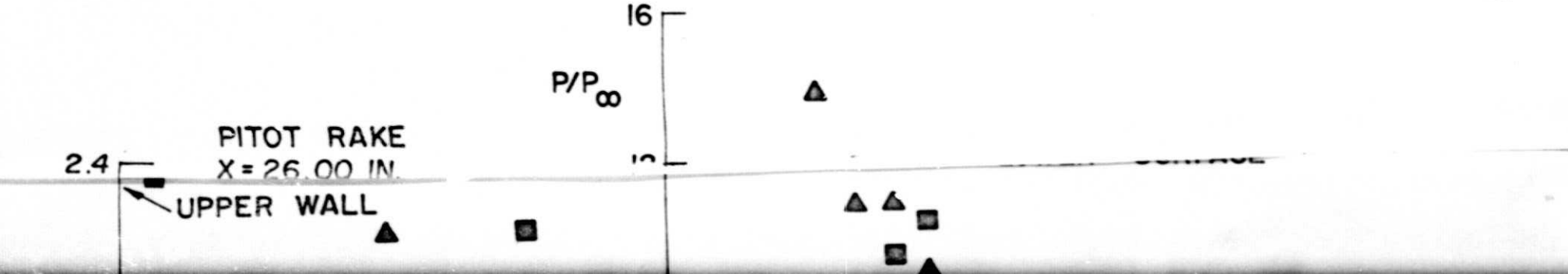

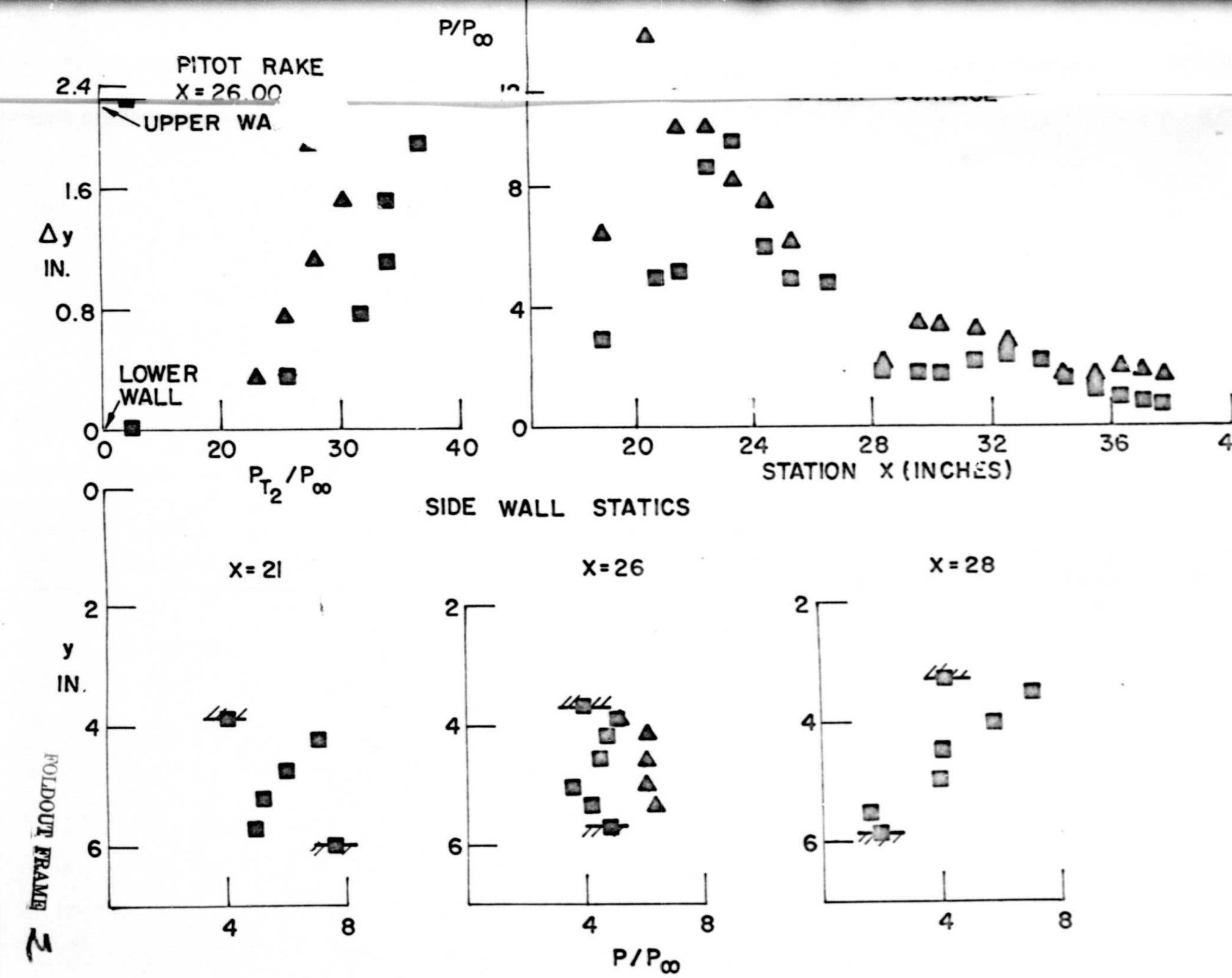

FOLDOUT FRAME 2

Fig. 41 Static pressure distributions with fuel injection through the lower freestream injector,

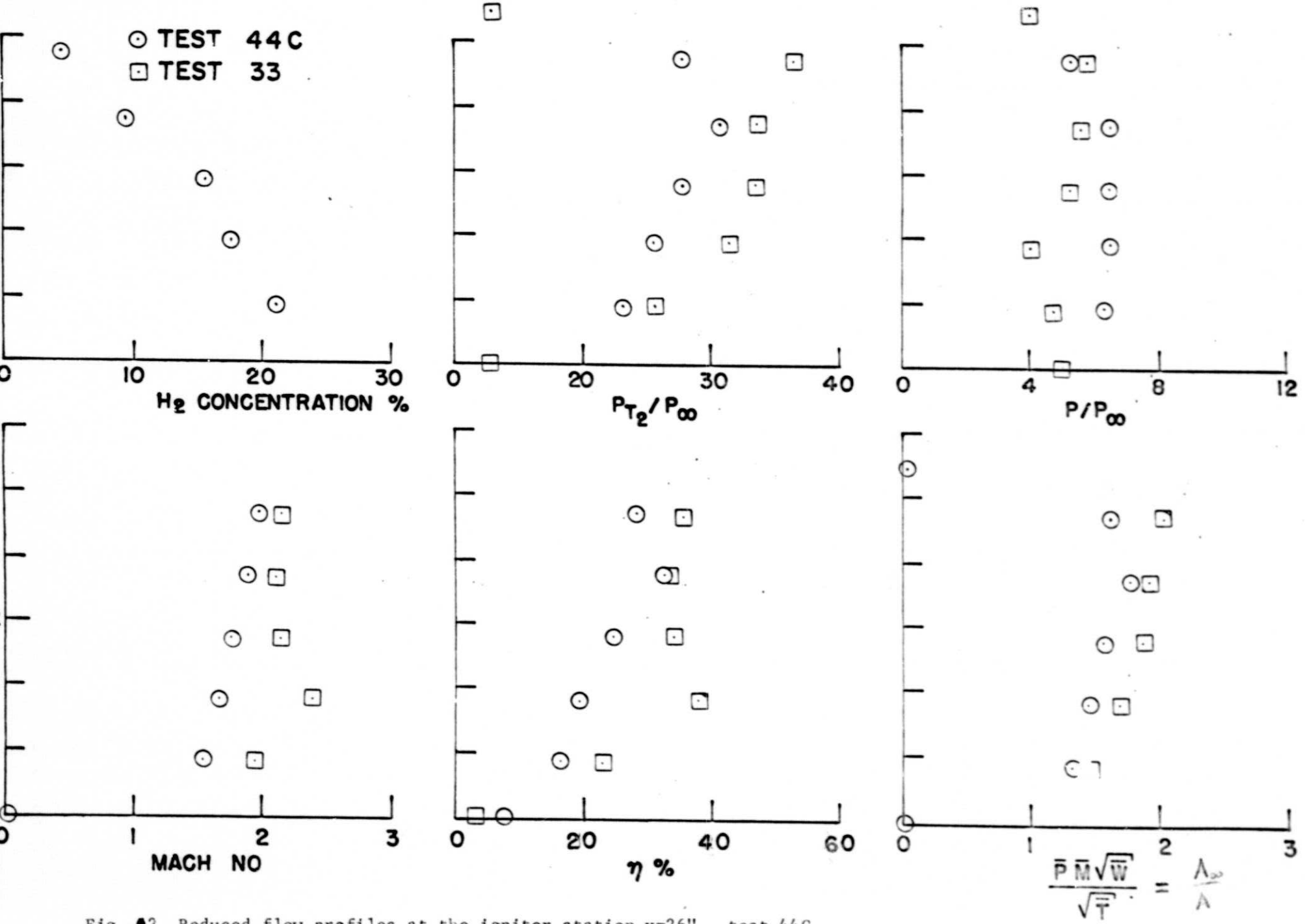

Fig. 12 Reduced flow profiles at the ignitor station x=26" - test 44C

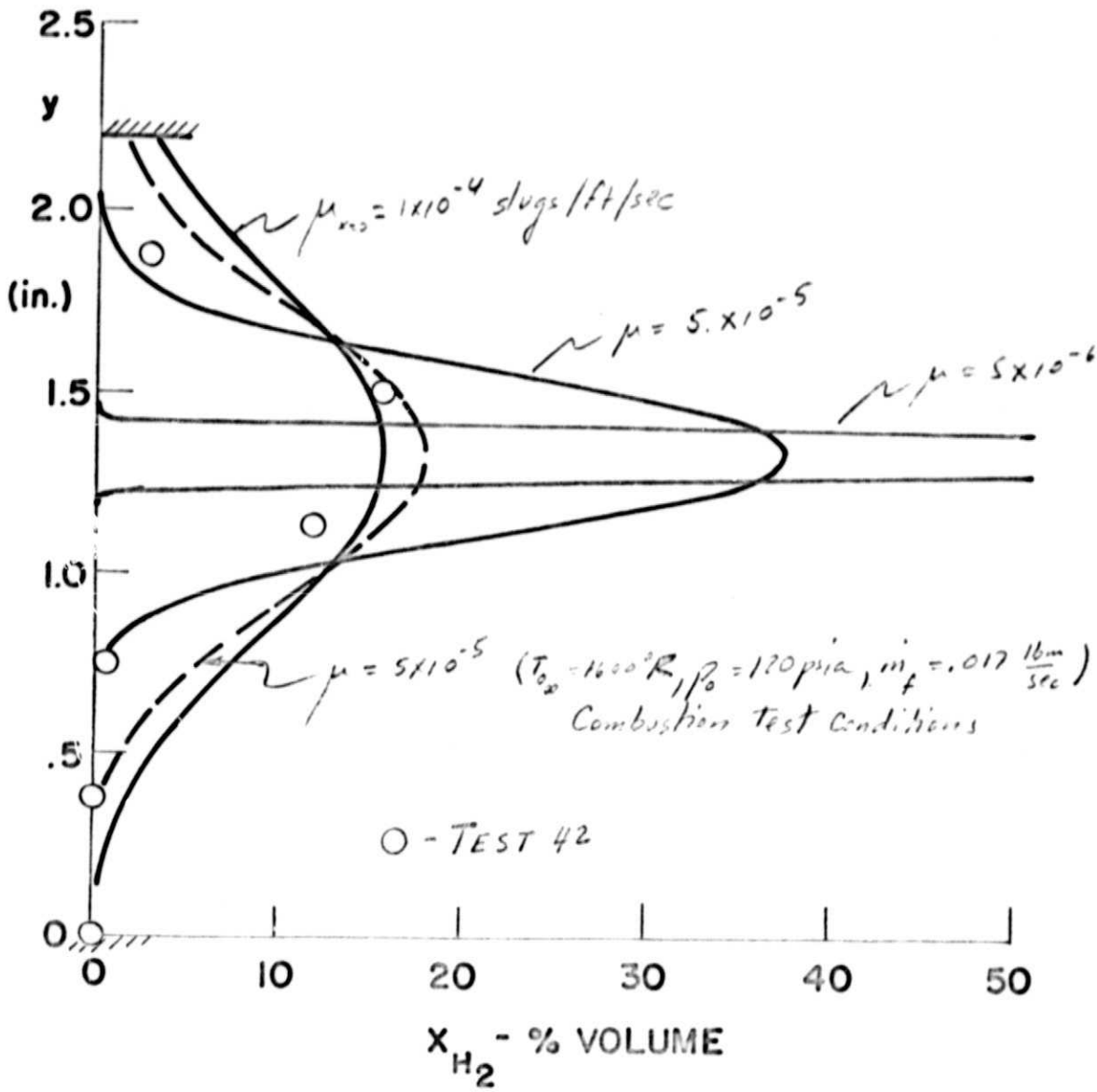

Fig. 3 Hydrogen concentration profile : the ignitor station x = 26" Fuel injection through the midstream injector only - $M_\infty = 4.0$, $T_o = 530^oR$, $p_o = 60$ psia, $m_f = .01$ lbm/sec

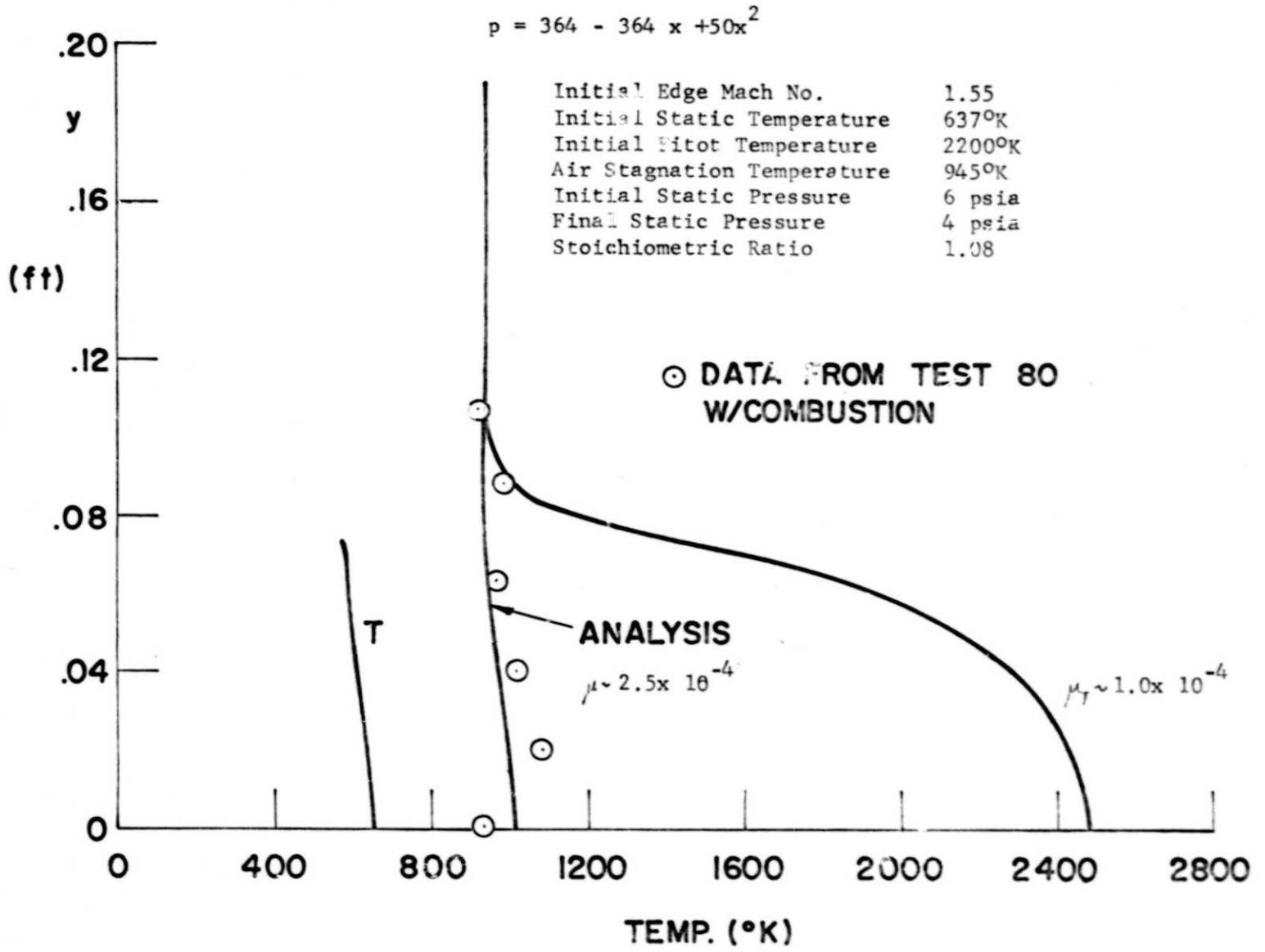

Fig. 4c Stagnation Temperature Profiles at the Combustor Exit ($x \simeq 0.9$ ft.)

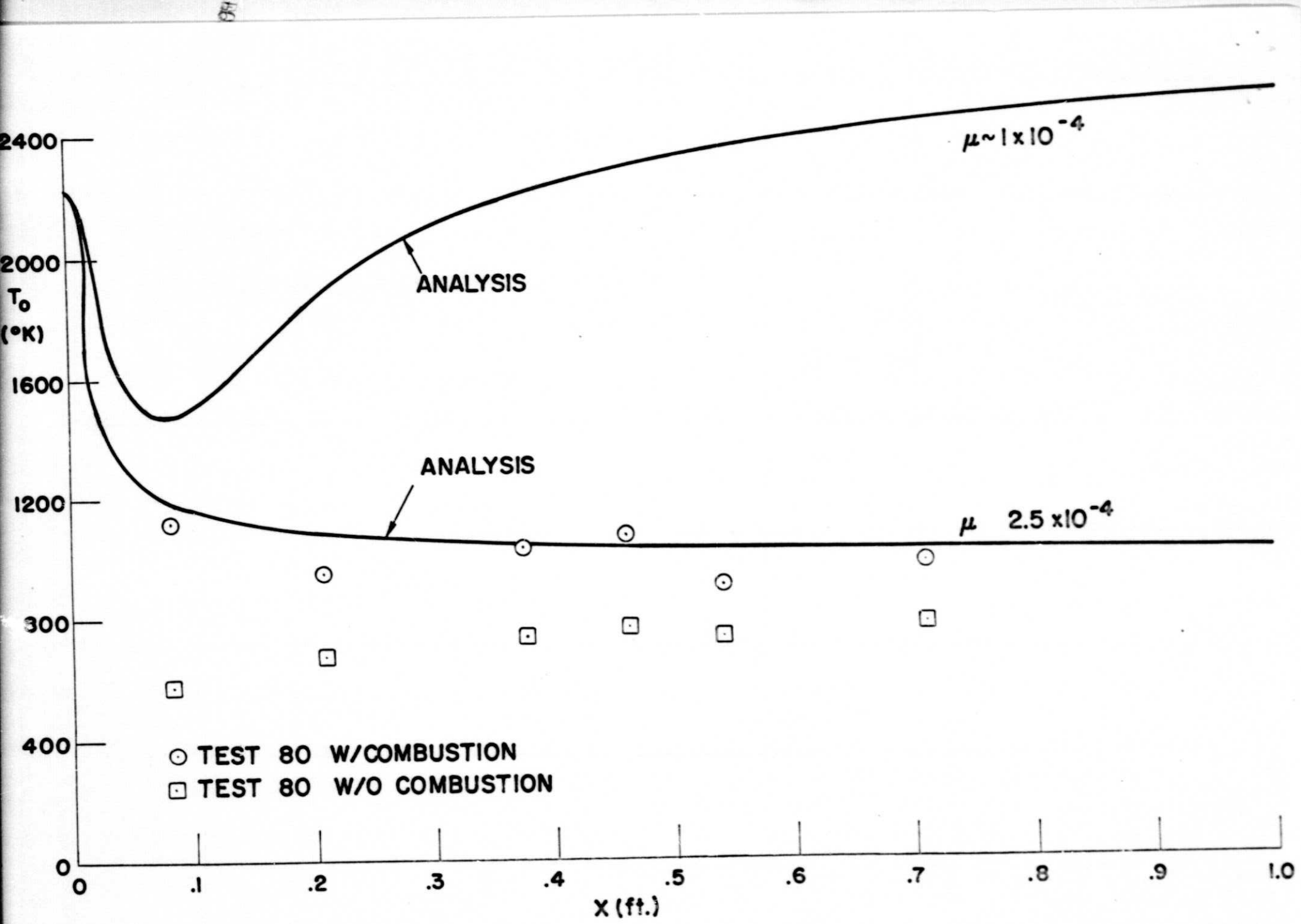

Fig. 4b Stagnation temperature variation along the lower wall of the combustor - $M_\infty = 4.0$

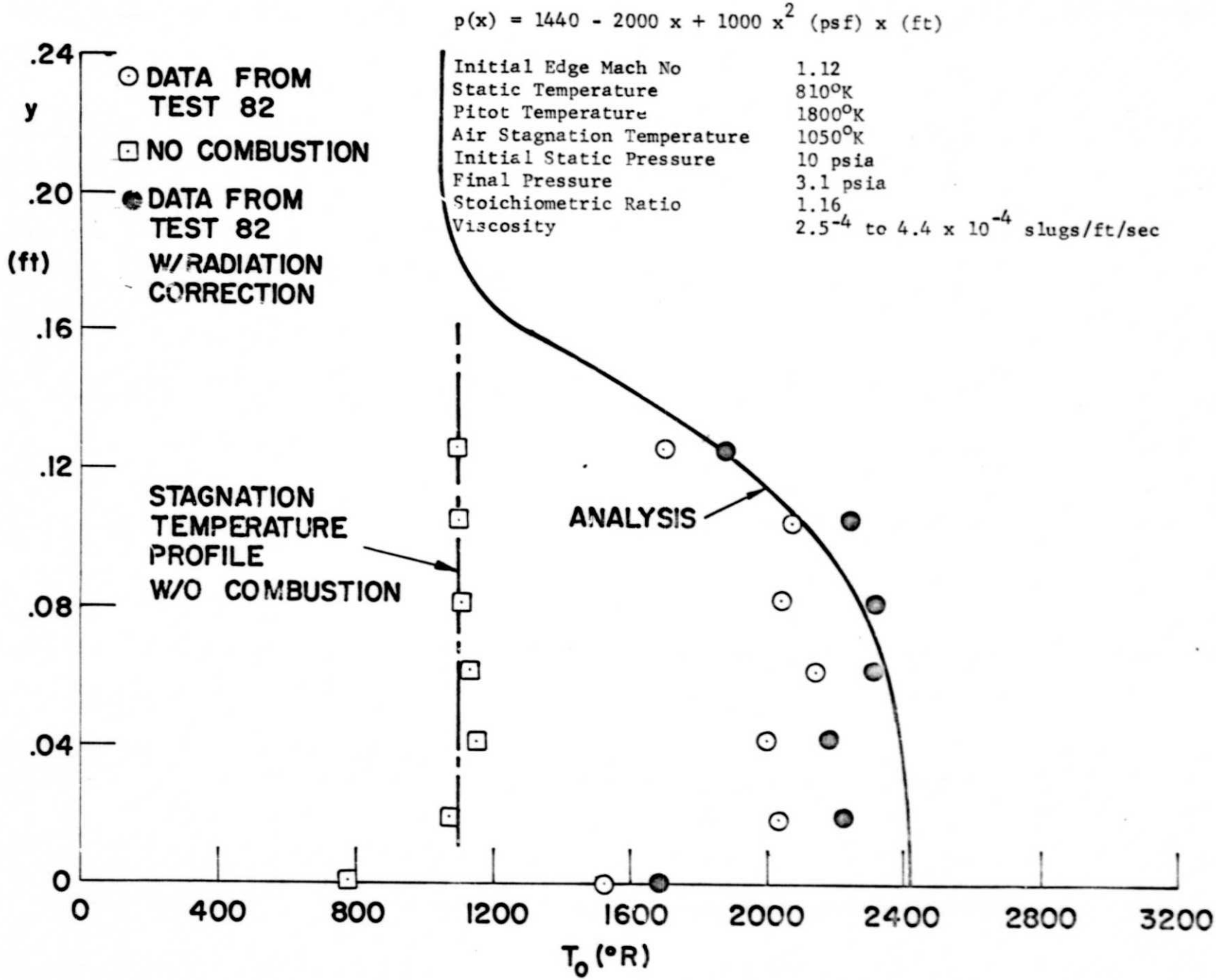

Fig. 5 Stagnation Temperature Profiles at the Combustor Exit (x = 0.9 ft.)

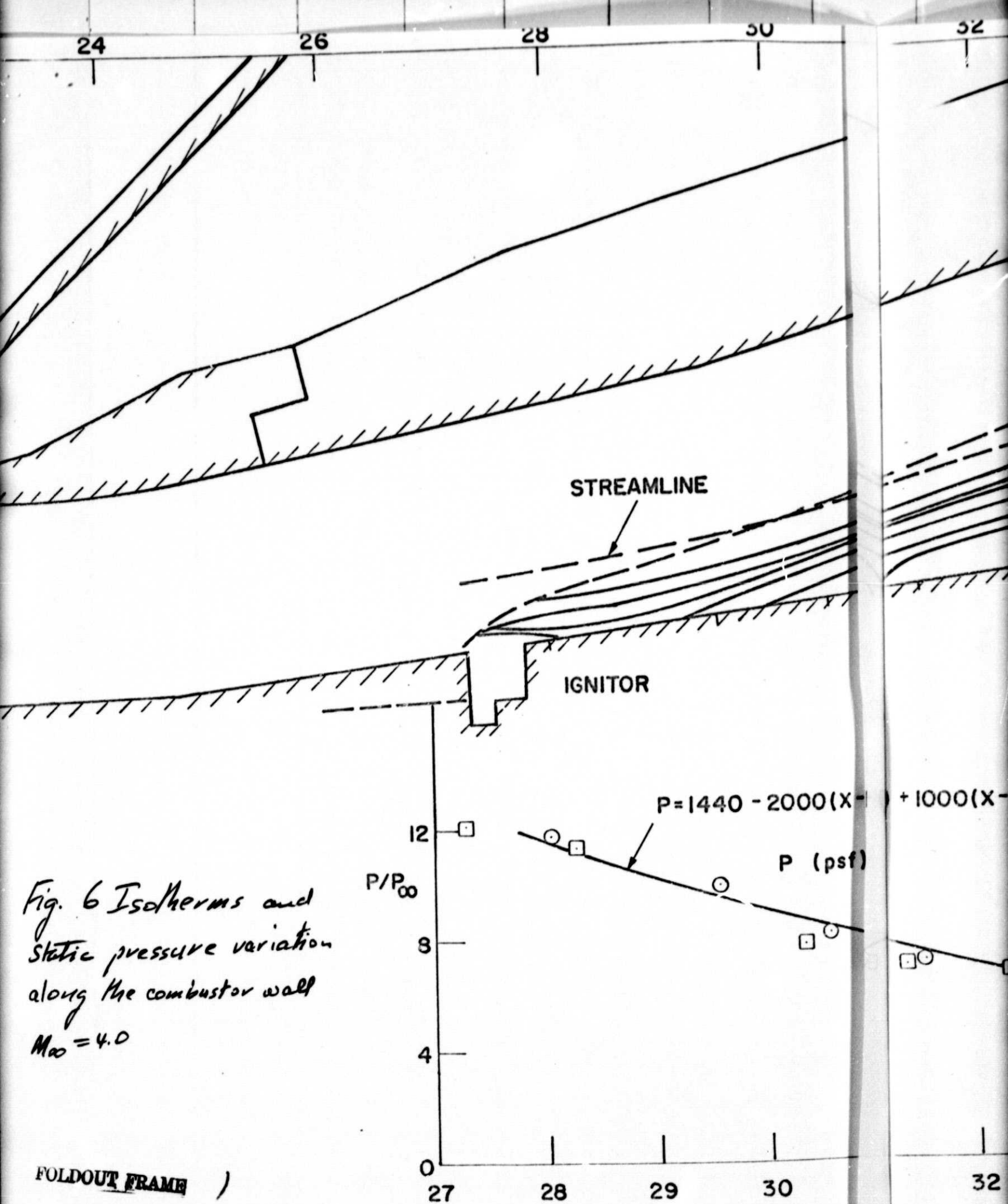

Fig. 6 Isotherms and static pressure variation along the combustor wall

$M_\infty = 4.0$

FOLDOUT FRAME)

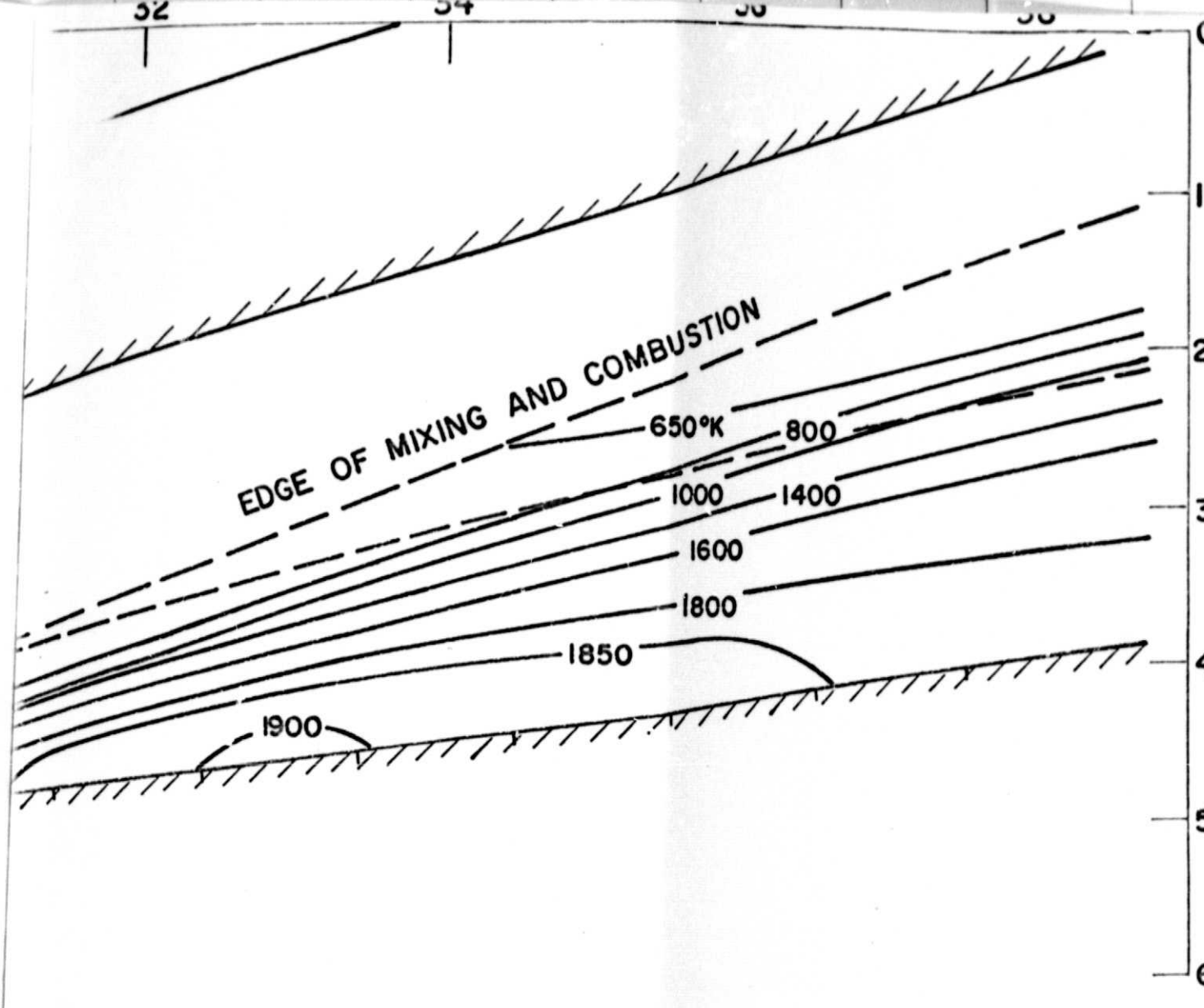

$+1000(X-X_o)^2$

⊙ LOWER SURFACE TEST 82
⊡ UPPER SURFACE

psf

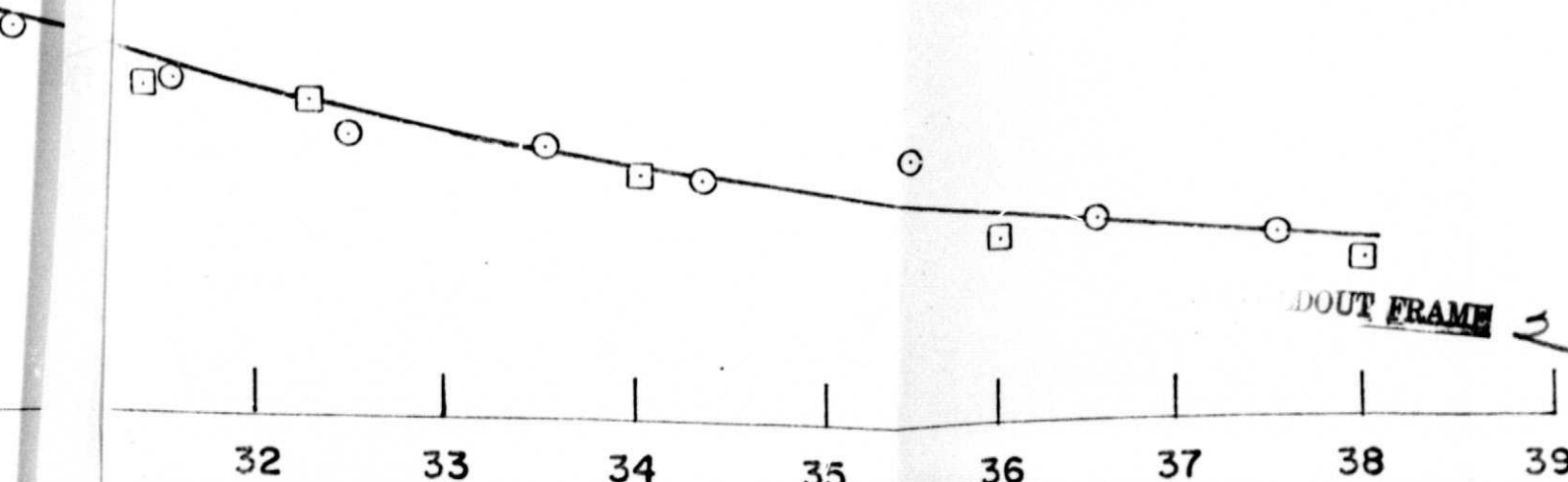

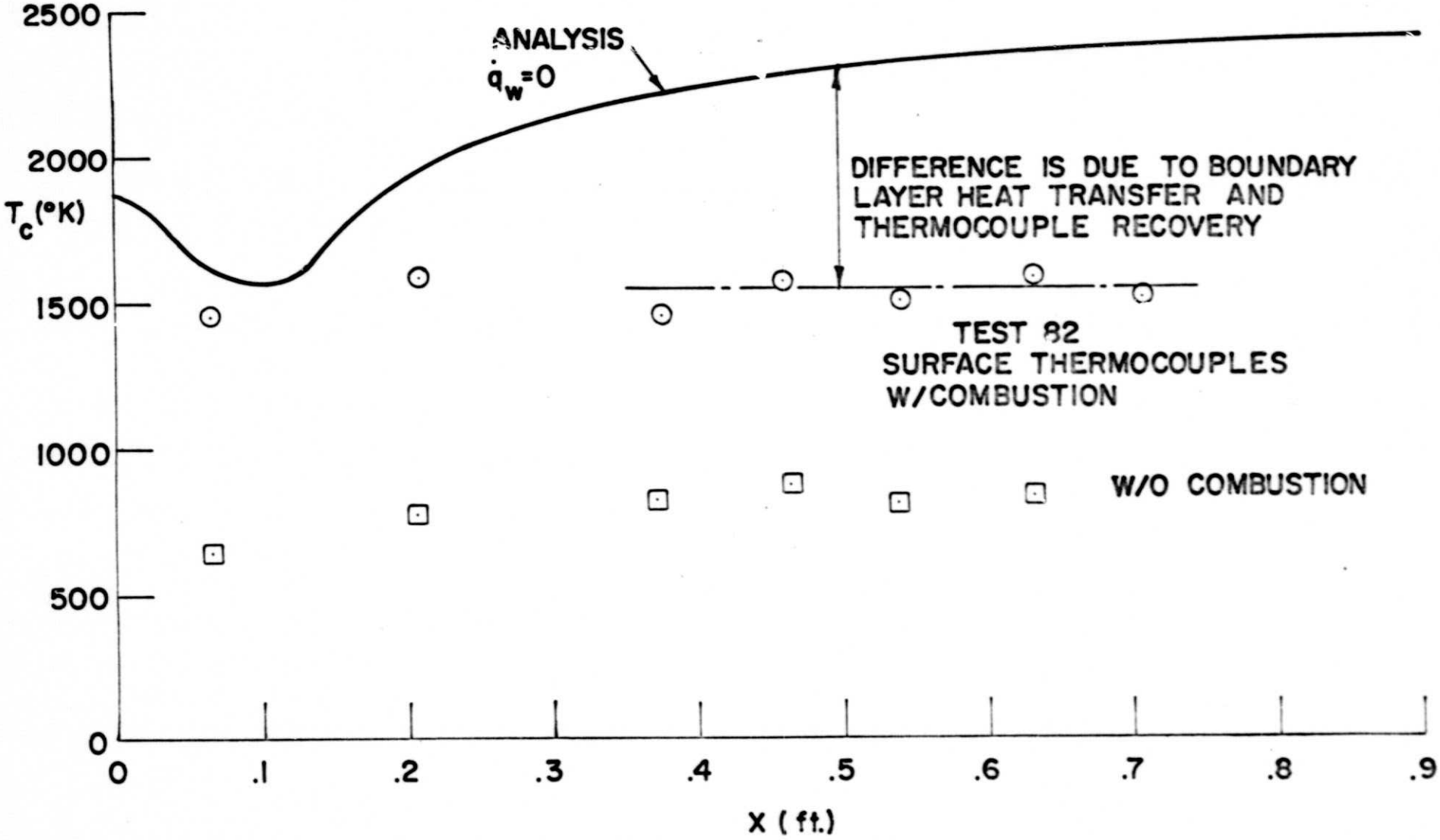

Fig. 7 Stagnation Temperature Variation along the lower Surface of the Combustor

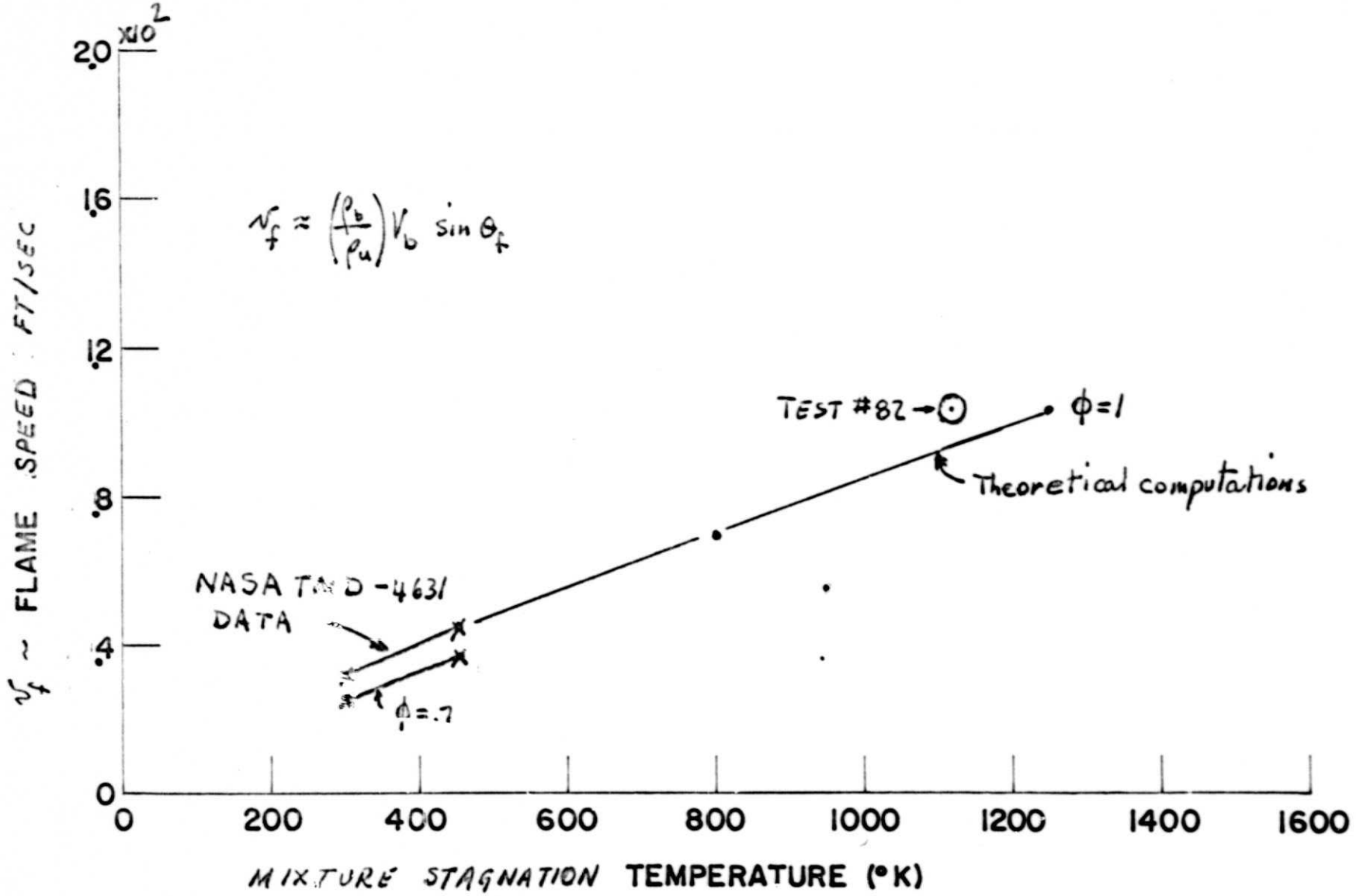

Fig. 8 Flame propagation velocity in premixed hydrogen-air systems